

# Description of a Storage Model for Phase Change Materials

Peter Puschnig

©August 31, 2004

## Contents

<b>1</b>	<b>Mathematical model</b>	<b>2</b>
1.1	Energy and mass conservation . . . . .	2
1.2	Multinode storage model – constant mass density . . . . .	4
1.3	Multinode storage model – varying mass density . . . . .	5
1.4	Energy exchange by direct double port connections . . . . .	6
1.5	Energy exchange by internal heat exchangers . . . . .	7
1.5.1	Energy balance . . . . .	7
1.5.2	The heat transfer coefficient . . . . .	8
1.6	Energy input by auxiliary heater . . . . .	11
1.7	Vertical heat conduction . . . . .	11
1.8	Losses to the ambient . . . . .	12
1.9	PCM modules . . . . .	12
1.9.1	Cylindrical Rods . . . . .	12
1.9.2	Heat transfer from the inner surface . . . . .	15
1.9.3	Heat transfer from the outer surface . . . . .	16
1.9.4	PCM Spheres . . . . .	17
<b>2</b>	<b>Description of the program interface</b>	<b>18</b>
2.1	Parameters . . . . .	19
2.2	Inputs . . . . .	21
2.3	Outputs . . . . .	21
<b>3</b>	<b>Simple Test Cases</b>	<b>22</b>
3.1	Losses to the ambient . . . . .	23
3.2	Heating by the built in auxiliary heater . . . . .	23
3.3	Loading the store by a double port . . . . .	23
3.4	Test system with three hydraulic connections . . . . .	23

# 1 Mathematical model

## 1.1 Energy and mass conservation

In this section we formulate the energy and mass conservation laws which build the basis of the subsequent sections where we will derive the actual equations describing the storage model keeping in mind that we want to model storage tanks involving media that undergo a phase change in the considered temperature range. Therefore, the specific heat capacity  $c_p$  will vary with temperature  $T$ , the same is of course true for the specific enthalpy  $q$ , the enthalpy per unit mass, which we will denote as

$$q = q(T). \quad (1)$$

For the following analysis this function may be any continuous and monotonously increasing function  $q = q(T)$ , thus employing the so called continuous property model (CPM) approach.

As an example Fig. 1 shows the temperature dependent specific enthalpies of water as well as for slurry with different PCM concentrations. The lower panel displays the corresponding specific heat capacities  $c_p = dq/dT$ . For the numerical simulation which will be described later on, the function  $q = q(T)$  can be provided by up to 100 data points  $T_i, q_i$ , where a linear interpolation scheme is used to compute  $q$  for arbitrary temperatures  $T$ . Due to the monotonously increasing behavior the function  $q = q(T)$  can be inverted to give  $T = T(q)$ . Concerning numerics, again a linear interpolation scheme will be used.

The change of enthalpy  $Q$  in a given control volume  $\Omega$  is given by the heat

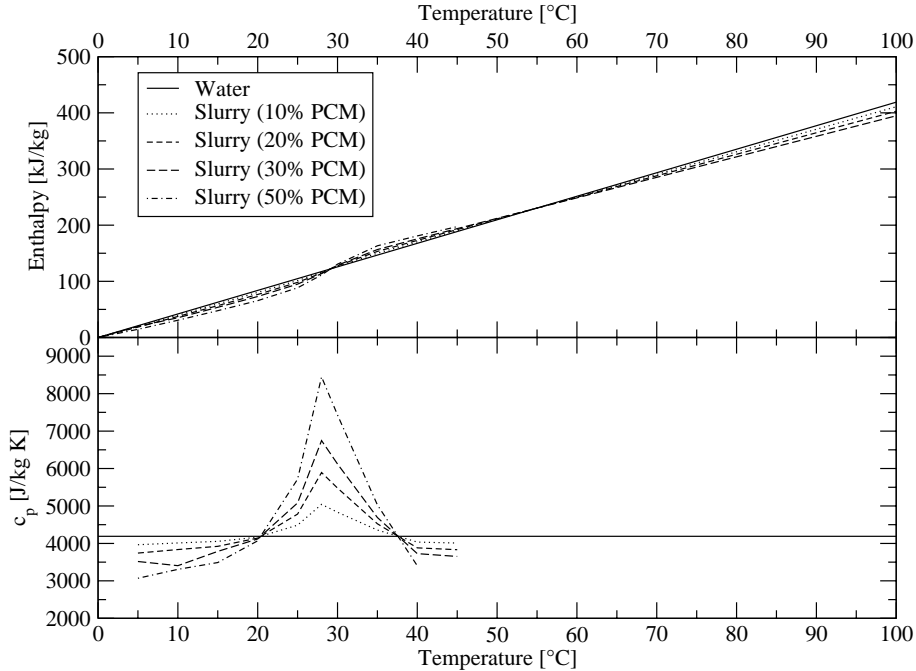


Figure 1: The temperature dependent enthalpy (top panel) and specific heat capacity (bottom panel) of water and slurry for different PCM concentrations.

current  $\mathbf{j}$  through the boundary surface  $\partial\Omega$ , by possible heat sources inside the volume with the power  $P$ , and by additional heat transition to the external to which the control volume may be coupled. The geometry is also indicated in Fig. 2. In a mathematical language, this can be expressed as

$$\frac{dQ}{dt} = \oint_{\partial\Omega} \mathbf{j} d\mathbf{A} + P + U_{\text{ext}} A (\bar{T} - T_{\text{ext}}) \quad (2)$$

In the last term of the above equation we have introduced the heat transfer coefficient  $U_{\text{ext}}$  to the external with the temperature  $T_{\text{ext}}$ . The heat current  $\mathbf{j}$  consists of two contributions, a conductive part governed by the thermal conductivity of  $\lambda$ , and a convective part determined by the velocity  $\mathbf{v}$ ,

$$\mathbf{j} = \lambda \nabla T + \rho q \mathbf{v}. \quad (3)$$

Here,  $\rho$  is the mass density, and  $q$  the specific enthalpy introduced above. Using the chain rule of differentiation the temperature gradient might also be expressed in terms of the gradient of the specific enthalpy and the specific heat capacity

$$\nabla T = \left( \frac{dq}{dT} \right)^{-1} \nabla q = \frac{\nabla q}{c_p}. \quad (4)$$

In addition to energy conservation we can also formulate a mass conservation law in the following form.

$$\frac{dM}{dt} = \oint_{\partial\Omega} \rho \mathbf{v} d\mathbf{A} \quad (5)$$

The total mass  $M$ , the total enthalpy  $Q$  and of the control volume  $\Omega$  are obtained from an integration over the control volume. The average temperature  $\bar{T}$  is follows from the average specific enthalpy  $\bar{q} = Q/M$  and the inverse of Eq. (1).

$$M = \int_{\Omega} d^3r \rho \quad (6)$$

$$Q = \int_{\Omega} d^3r \rho q \quad (7)$$

$$\bar{T} = T(\bar{q}) \quad (8)$$

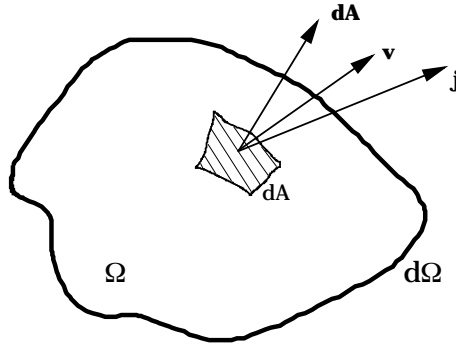


Figure 2: The control volume  $\Omega$  with its boundary surface  $\partial\Omega$ . The heat flow vector  $\mathbf{j}$ , the velocity  $\mathbf{v}$ , and the surface element  $d\mathbf{A}$  are indicated.

So far we allowed the density  $\rho$  to depend on the temperature  $T$ . If we, however, assume this dependence to be negligible, thus  $\rho = \rho_c \neq \rho(T)$  the formulae given above can be considerably simplified. Most importantly, the mass conservation (5) simplifies to  $M = \text{const}$  since the density on the right hand side of Eq. (5) can be put outside of the integral and the closed surface integral of the source-free vector field  $\mathbf{v}$  vanishes. Due to the constant density the energy and mass conservation equations decouple, where the mass equation is trivially fulfilled and the density appears only as simple multiplication factor in the energy equation. In the following sections the presumption of constant mass density will be made.

## 1.2 Multinode storage model – constant mass density

In the multinode approach, the tank is modeled as  $N$  fully mixed volume segments (nodes) which is depicted schematically in Fig. 3. Thus, the geometry of each control volume – in the language of Fig. 2 – is a cylinder of height  $\Delta z$  and top and bottom surface area  $A$ . Each node is characterized by its mass  $m_j$ , its specific enthalpy  $q_j$ , and its temperature  $T_j$ . In fact, for a given fluid the temperature  $T$  is a unique function of the enthalpy  $q$  and vice versa. If we assume a temperature independent mass density, thus  $\rho \neq \rho(T)$ , then the node masses  $m_j$  are constant. In this case, the energy balance of the  $j$ -th storage

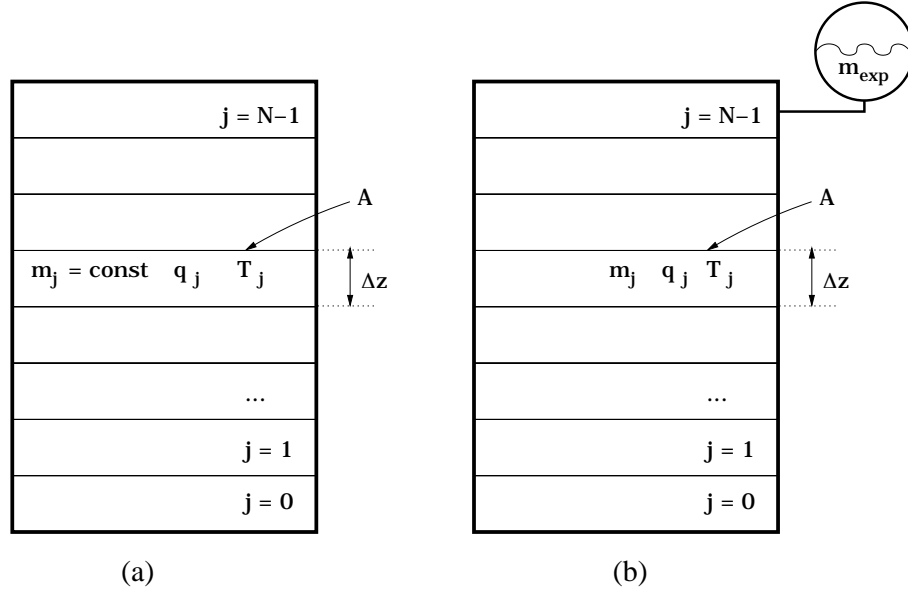


Figure 3: The multinode storage model with  $N$  nodes each consisting of a cylindrical volume with height  $\Delta z$  and top and bottom surface  $A$ . If the mass density is a constant  $\rho \neq \rho(T)$ , then the node masses  $m_j$  are constant (a), otherwise an expansion vessel is needed in order to compensate for the varying density (b).

node might be written in the following form:

$$m_j \frac{dq_j}{dt} = \dot{Q}_j^{(\text{dp})} + \dot{Q}_j^{(\text{hx})} + \dot{Q}_j^{(\text{aux})} + \dot{Q}_j^{(\text{cond})} + \dot{Q}_j^{(\text{loss})} + \dot{Q}_j^{(\text{PCM})} \quad (9)$$

Here, the superscripts denote the enthalpy change due to loading or discharging by double port connections (dp), internal heat exchangers (hx), energy input by a built-in auxiliary heater (aux), heat conduction to neighboring nodes (cond), losses to the ambient (loss), and finally heat exchange between the storage fluid and possible PCM modules inside the storage tank (PCM). Compared to the energy conservation (2) the left hand side of (9) already assumes constant mass density. The terms on the right hand side arise from conductive heat flow (cond), convective heat flow (dp), heat transfer to an external domain (hx, loss, PCM), and internal heat sources (aux). Each of these contributions can be derived from Eq. (2) and will be discussed in the following sections. The resulting formulae are given by Eqs. (13), (17), (32), (33), (35), and (37).

Numerically, the time evolution of (9) is solved by the explicit method,

$$q_j(t + \Delta t) = q_j(t) + \frac{\Delta t}{m_j} \sum \dot{Q}_j(t). \quad (10)$$

Here, the right hand side only contains quantities at time  $t$ , thus the new enthalpy of node  $j$  at time  $t + \Delta t$  is *explicitly* given by quantities only at the old time  $t$ .

### 1.3 Multinode storage model – varying mass density

In this section we want to discuss the necessary changes in the model if we allow the mass density  $\rho$  to be a function of the temperature  $T$ . First of all, since the storage medium is assumed to be incompressible, a temperature dependent density leads results in a varying mass in the storage tank which has to be compensated for by an expansion vessel as can be seen from the right part of Fig. 3. Thus, the total mass of the system  $M$  including the masses of the storage nodes  $m_j$  plus the mass in the expansion vessel  $m_{\text{exp}}$ ,

$$M = \sum_{j=0}^{N-1} m_j + m_{\text{exp}} = \text{const.} \quad (11)$$

The change in enthalpy  $Q_j = V_j \rho_j q_j$  of the storage node  $j$  is now given by

$$\frac{dQ_j}{dt} = V_j \frac{dq_j}{dt} \left[ q_j \frac{d\rho_j}{dq_j} + \rho_j \right]. \quad (12)$$

Here, the first term in brackets accounts for changes in density  $\rho$  upon temperature, or equivalently, specific enthalpy  $q_j$ . If this term were zero, then the equation would turn into the simple form discussed in the previous section.

The time evolution of the coupled energy and mass conservation laws, Eqs. (2) and (5), can now be solved according to the following computational steps:

- (i) At time  $t$ , the mass  $m_j$ , the specific enthalpy  $q_j$  is known for each storage node. Also from  $Q = mq$ , the total enthalpy  $Q_j$ , from  $T = T(q)$  the temperature  $T_j$ , and from  $\rho = m/V$  the mass density  $\rho_j$  is given.

- (ii) The solution of the energy conservation equation (2) results in the enthalpy  $Q_j(t + \Delta t)$  of node  $j$  at the new time step.
- (iii) Eq. (12) yields the specific enthalpy  $q_j(t + \Delta t)$  and by application of the relation  $T = T(q)$  the new temperatures  $T_j(t + \Delta t)$  are obtained. Moreover, the density  $\rho_j$  follows from  $\rho = \rho(T)$ , and therefore also the new masses  $m_j(t + \Delta t)$ .
- (iv) The mass conservation (5) finally results in the mass  $m_{\text{exp}}$  in the expansion vessel as well as in the convective velocities due to thermal expansion. Thus, all necessary quantities at time  $t + \Delta t$  are known, and the computation can proceed to the next time step.

#### 1.4 Energy exchange by direct double port connections

The current model allows up to five double port connections. For each double port  $p$ , the inlet flow rate  $\dot{m}_p^{(\text{in})}$  and the specific enthalpy  $q_p^{(\text{in})}$  of the fluid at the inlet determines the enthalpy change of storage node  $j$  in the following way

$$\dot{Q}_j^{(\text{dp})} = \sum_p \dot{m}_p^{(\text{in})} \left[ \left( q_p^{(\text{in})} - q_j \right) \delta_{i_p j} + \left( q_{j+d_p} - q_j \right) \epsilon_{i_p j o_p} \right]. \quad (13)$$

Here,  $i_p$  and  $o_p$ , respectively, denote store node indices at the inlet and outlet of port  $p$  as can be seen from Fig. 4. The Kronecker delta  $\delta_{i_p j}$  is defined in the usual way,

$$\delta_{i_p j} = \begin{cases} 1 & \text{if } i_p = j \\ 0 & \text{if } i_p \neq j \end{cases} \quad (14)$$

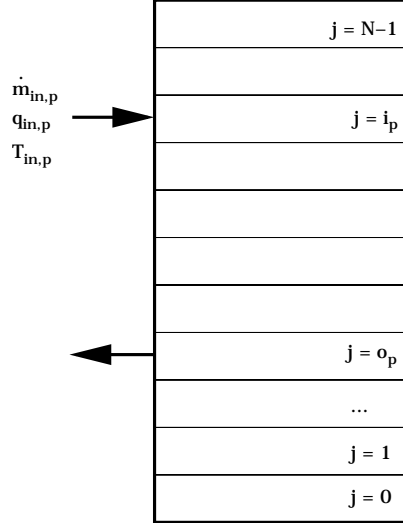


Figure 4: Multinode storage model with direct double port connection  $p$ . The inlet flow rate is denoted by  $\dot{m}_p^{(\text{in})}$ ,  $q_p^{(\text{in})}$  is the specific enthalpy of the inlet flow, and  $T_p^{(\text{in})}$  its corresponding temperature.

The direction flow parameter  $d_p$  and the factor  $\epsilon_{i_p j o_p}$  are defined in the following way:

$$d_p = \begin{cases} +1 & \text{if } i_p \geq o_p \\ -1 & \text{if } i_p < o_p \end{cases} \quad (15)$$

$$\epsilon_{i_p j o_p} = \begin{cases} 1 & \text{if } 0 < d_p (i_p - j) \leq d_p (i_p - o_p) \\ 0 & \text{else.} \end{cases} \quad (16)$$

## 1.5 Energy exchange by internal heat exchangers

### 1.5.1 Energy balance

Node  $j$  of the internal heat exchanger  $p$  is characterized by its mass,  $m_j^{(p)}$ , its specific enthalpy  $q_j^{(p)}$ , and  $T_j^{(p)}$  its corresponding temperature. The heat transfer rate between heat exchanger node  $j$  and storage node  $j$  is denoted by  $(UA)_j^{(p)}$ . With these conventions, the energy change of storage node  $j$  due to the internal heat exchanger is given by

$$\dot{Q}_j^{(\text{hx})} = - \sum_p (UA)_j^{(p)} [T_j - T_j^{(p)}]. \quad (17)$$

Note that the store node temperatures  $T_j$  as well as the heat exchanger node temperatures  $T_j^{(p)}$  can be obtained from the function  $T = T(q)$  for a given fluid. The heat exchanger energy balance which determines the required enthalpies  $q_j^{(p)}$  and temperatures  $T_j^{(p)}$  can be written in the following form

$$\begin{aligned} m_j^{(p)} \frac{dq_j^{(p)}}{dt} &= \dot{m}_p^{(\text{in})} \left[ \left( q_p^{(\text{in})} - q_j^{(p)} \right) \delta_{i_p j} + \left( q_{j+d_p}^{(p)} - q_j^{(p)} \right) \epsilon_{i_p j o_p} \right] \\ &- (UA)_j^{(p)} [T_j^{(p)} - T_j]. \end{aligned} \quad (18)$$

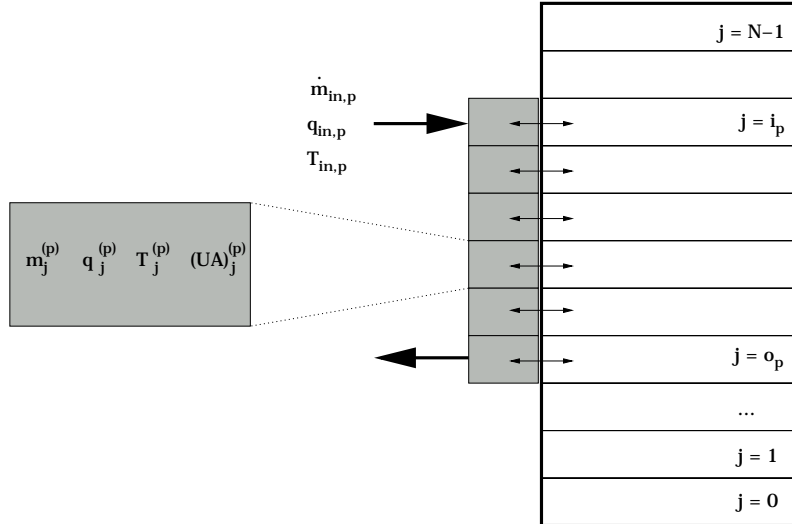


Figure 5: Multinode storage model with internal heat exchanger.

Here, the first describes the energy exchange in the internal heat exchanger nodes due to the inlet flow at flow rate  $\dot{m}_p^{(\text{in})}$  and specific enthalpy  $g_p^{(\text{in})}$ . Thus it is equivalent to Eq. (13) using the same definitions from Eq. (14)–(16). The second term in Eq. (18) is equivalent to the term of Eq. (17) and handles the energy exchange between internal heat exchanger and store nodes. It is understood that for nodes  $j$  outside the in- and outlets there is no heat transfer to the store nodes. Mathematically, this might be expressed in the way that  $(UA)_j^{(p)} = 0$  if  $d_p(j - i_p) > 0$  or  $d_p(j - o_p) < 0$ . Note that we assumed *no* losses of the heat exchanger to the ambient, and the vertical conduction between heat exchanger nodes has been neglected.

### 1.5.2 The heat transfer coefficient

In the previous section, the heat transfer coefficient  $(UA)_j^{(p)}$  has only been introduced as a parameter. Here we attempt to calculate this quantity for a helical pipe heat exchanger from the hydrodynamic flow conditions inside and outside of the heat exchanger tube. Figure 6 shows a cross section through a helical tube heat exchanger with inner and outer pipe radii  $r_i$  and  $r_o$ , respectively. The temperature of the fluid inside of the heat exchanger pipe is given by  $T_{\text{hx}}$ , the storage fluid temperature is  $T_{\text{store}}$ , and the surface temperatures at the inner and outer surface of the pipe are denoted by  $T_{s,i}$  and  $T_{s,o}$ , respectively. The overall heat resistance may be expressed as [1]

$$R_{\text{tot}} = \frac{1}{h_i 2\pi r_i L} + \frac{\ln(r_o/r_i)}{2\pi\lambda L} + \frac{1}{h_o 2\pi r_o L}, \quad (19)$$

where the heat transfer coefficients  $h_i$  and  $h_o$  for the inner and outer surface have been introduced, and  $\lambda$  denotes the thermal conductivity of the pipe material.

For the computation of  $h_i$  we are facing an internal flow condition in a cylindrical pipe where the flow velocity  $v$  is determined by the mass flow rate  $\dot{m}$  through the heat exchanger and its inner cross section  $D_i = 2r_i$ . The Reynolds number  $Re$  can be written in the following way

$$Re = \frac{4}{\pi} \frac{\dot{m}}{D_i \mu} \quad (20)$$

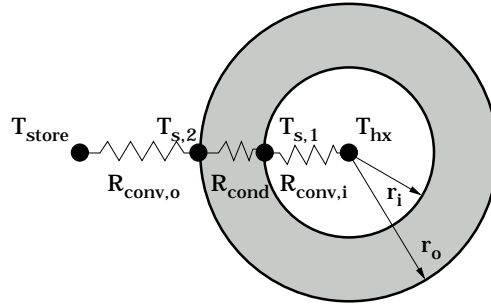


Figure 6: Cross section through a helical tube heat exchanger with inner and outer pipe radii  $r_i$  and  $r_o$ , respectively.



where  $\mu$  is the dynamic viscosity. In order to give a numerical example, we take water at 320 K,  $\mu = 0.577 \times 10^{-3}$  [Ns/m<sup>2</sup>],  $\dot{m} = 500$  [kg/h], and a pipe diameter  $D_i = 1$  [cm], resulting in  $Re = 30648$  which clearly shows that the flow conditions are expected to be turbulent for this example. Whether the flow is in the laminar or in the turbulent regime, however, has to be checked for a given situation. The desired heat transfer coefficient is related to the Nusselt number  $Nu$  via the relation

$$h_i = \frac{\lambda Nu_D}{D_i}. \quad (21)$$

Several relations for the  $Nu$  number for laminar as well as for the turbulent case can be found in the literature [2, 3]

$$Nu_D = \frac{(f/8)Re_D Pr}{1.07 + 12.7(f/8)^{1/2}(Pr^{2/3} - 1)} \quad (22)$$

$$(0.5 < Pr < 2000) \wedge (10^4 < Re_D < 5 \times 10^6)$$

$$Nu_D = \frac{(f/8)(Re_D - 1000)Pr}{1 + 12.7(f/8)^{1/2}(Pr^{2/3} - 1)} \quad (23)$$

$$(0.5 < Pr < 2000) \wedge (3000 < Re_D < 5 \times 10^6)$$

Here,  $Pr$  denotes the Prandtl number and  $f$  is the friction factor which for smooth pipes and values of  $3000 < Re_D < 5 \times 10^6$  is given by [2]

$$f = (0.790 \times \ln Re_D - 1.64)^{-2}. \quad (24)$$

For the example given above, the Prandtl number is  $Pr = 3.77$ , and the friction factor is given by  $f = 0.0235$ . Then from the first relation [2] we have  $Nu_D = 165.7$ , and from the second [3]  $Nu_D = 165.9$ . The insertion into (21) gives  $h_i = 10620$  [W/m<sup>2</sup>K] or  $h_i A_i = 333$  [W/K] and meter pipe length.

For the evaluation of the outer heat transfer coefficient  $h_o$  we take two different approaches. In the first, we treat the exchanger pipe as a horizontal cylinder with radius  $r_o$  that is subjected to free convection due to a density gradient in the surrounding store medium. For such a geometry, an expression for the Nusselt number can be derived for free convection around a horizontal cylinder [4]

$$Nu_D = \left\{ 0.60 + \frac{0.387 Ra_D^{1/6}}{\left[ 1 + (0.559/Pr)^{9/16} \right]^{8/27}} \right\}^2 \quad (25)$$

This relation is valid for Rayleigh numbers  $Ra_D < 10^{12}$  where the  $Ra_D$  is given by

$$Ra_D = \frac{g\beta(T_{s,o} - T_{store})D_o^3}{\nu\alpha}. \quad (26)$$

Here,  $g$  denotes the gravitational acceleration,  $\beta$  is the volumetric thermal expansion coefficient

$$\beta = -\frac{1}{\rho} \left( \frac{\partial \rho}{\partial T} \right)_p, \quad (27)$$

and  $\nu$  and  $\alpha$ , respectively are the kinematic viscosity and the thermal diffusivity. The previously unknown surface temperature  $T_{s,o}$  entering the calculation of

$Ra_D$  has to be determined in an iterative procedure. Starting from an initial guess for the outer surface temperature,  $h_o$  can be computed and together with the inner heat transfer coefficient  $h_i$  the total thermal resistance (19) as well as the outer convection resistance  $R_{\text{conv},o}$  are determined. Thus from

$$T_{s,o} = T_{\text{store}} + \frac{R_{\text{conv},o}}{R_{\text{tot}}} (T_{\text{hx}} - T_{\text{store}}) \quad (28)$$

a new value for the outer surface temperature can be obtained and the iteration completed. We close this section by giving a numerical example for the calculation of the total heat transfer coefficient for the internal heat exchanger. The contribution of the inner surface convection has already been computed to be  $h_i A_i = 333$  [W/K] and meter pipe length. Assuming a pipe wall thickness of 5 [mm], thus  $D_o = 0.015$  [m], and a thermal conductivity of the pipe wall of  $\lambda_{\text{pipe}} = 400$  [W/mK], the thermal resistance is given by  $LR_{\text{pipe}} = 1/6200$  [mK/W]. For the outer heat transfer coefficient, we assume a storage temperature  $T_{\text{store}} = 290$  [K] and start the iterative computation with an initial guess  $T_{s,o}^{(1)} = 310$  [K] for the outer pipe surface temperature. Then, the film temperature  $T_f$  at which the thermophysical properties has to be evaluated is given by  $T_f^{(1)} = 1/2(T_{\text{store}} + T_{s,o}^{(1)}) = 300$  [K]. Using the thermophysical properties of water taken from [1] at 300 [K], Eq. (26) yields  $Ra_D = 1.455 \times 10^6$ , and Eq. (25)  $Nu_D = 6.7$ . Then from (19) we have

$$LR_{\text{tot}} = \frac{1}{333} + \frac{1}{6200} + \frac{1}{12.9} = \frac{1}{12.2} [\text{mK/W}] \quad (29)$$

where the first term is the contribution heat transfer at the inner surface, the second accounts for the pipe heat conduction, while the third results from the heat transfer at the outer pipe surface. Clearly, the dominating part is the outer heat transfer. For the second iteration we calculate the new surface temperature  $T_{s,o}^{(2)}$  according to (28) to be  $T_{s,o}^{(2)} = 318.4$  [K]. Using the thermophysical properties at the new film temperature  $T_f^{(2)} = 304.2$  [K],  $Ra_D = 2.62 \times 10^6$  and  $Nu_D = 17.2$ , thus  $LR_{\text{conv},o} = 1/33.6$  [mK/W]. And from (19) the total heat transfer coefficient is given by 29.7 [W/mK]. At this point we want to stop the iteration procedure in this numerical example though the the results are not yet fully converged.

As an alternative way to calculate the outer heat transfer coefficient  $h_o$  we attempt to model the free convection over the entire height of internal heat exchanger. This model is based on the Grashoff number given by

$$Gr_z = \frac{g\beta(T_{s,o} - T_{\text{store}})z^3}{\nu^2}. \quad (30)$$

Here,  $z$  denotes the vertical position in the storage tank. Due to the  $z^3$  dependence the Grashoff number, and hence the heat transfer coefficient, will be much higher at the top of the store as compared to the bottom. The heat transfer coefficient is determined from the following empirical relation

$$h_o(z) = \xi Gr_z^{\frac{1}{4}}, \quad (31)$$

where  $\xi$  is an empirical constant for a given store and heat exchanger geometry and has to be determined from comparison with experiments. The quantity  $\xi$

has the units of a heat transfer coefficient and might also be interpreted as  $\xi = \lambda/l_{\text{char}}$ , where  $\lambda$  is the thermal conductivity of the storage medium and  $l_{\text{char}}$  is a characteristic convection length for the given storage / heat exchanger geometry.

In the actual computation, the method by which the heat transfer coefficient will be calculated can be determined by a parameter  $P$  (for instance, PORT1 parameter 28). There are three possibilities

- (i)  $P > 0$ : The total heat transfer coefficient is a *constant* given by  $P$  in [W/mK]
- (ii)  $P = 0$ : The inner heat transfer coefficient  $h_i$ , and the pipe resistance will be computed according to the formulae outlined in this section. The outer heat transfer coefficient  $h_o$  is calculated from the *horizontal cylinder* approach.
- (iii)  $P < 0$ : Again, the inner heat transfer coefficient  $h_i$ , and the pipe resistance will be computed according to the formulae outlined in this section. In this mode, the outer heat transfer coefficient  $h_o$  is calculated from the *Grashoff* ansatz mentioned above, where the empirical parameter  $\xi$  is set to the  $|P|$  [W/m<sup>2</sup>K].

## 1.6 Energy input by auxiliary heater

The energy input into the storage node  $j$  by a built-in electrical heater is given by

$$\dot{Q}_j^{(\text{aux})} = P_j^{(\text{aux})} = \frac{P^{(\text{aux})}}{n^{(\text{aux})}}, \quad (32)$$

where  $P^{(\text{aux})}$  is the total power of the auxiliary heater and  $n^{(\text{aux})}$  is the number of storage nodes covered by the auxiliary heater. Again it is understood that above equation is only relevant for storage nodes inside the range of the auxiliary.

## 1.7 Vertical heat conduction

The energy change due to heat conduction to neighboring storage nodes is governed by the following expression

$$\dot{Q}_j^{(\text{cond})} = \lambda_{\text{eff}} \frac{A}{\Delta z} [T_{j+1} - 2T_j + T_{j-1}]. \quad (33)$$

Here,  $A$  is the cross section of the storage tank,  $\Delta z$  is the thickness of one storage node, and  $\lambda_{\text{eff}}$  is an effective thermal conductivity. This value includes the effects of thermal conduction due to the storage medium as well as heat conduction due to storage walls and constructions inside the tank such as internal heat exchangers.

We note that the Eq. (33) only applies if the density variations of the storage fluid are neglected. If we allow for a temperature dependent mass density  $\rho = \rho(T)$  as outlined in Sec. 1.3, then the convective part of the heat flux of Eq. (3) leads to an additional term

$$\dot{Q}_j^{(\text{conv})} = \dot{\rho}_j V_j q_j, \quad (34)$$

where  $\dot{\rho}_j$  accounts for the density change in node  $j$  due to temperature variations.

## 1.8 Losses to the ambient

Heat losses of the storage tank to the ambient at temperature  $T_{\text{amb}}$  are governed by

$$\dot{Q}_j^{(\text{loss})} = -(UA)_j^{(\text{amb})} [T_j - T_{\text{amb}}]. \quad (35)$$

The heat transfer coefficient of  $(UA)_j^{(\text{amb})}$  of node  $j$  can be obtained from the overall heat loss coefficient of the storage tank  $(UA)^{(\text{amb})}$  by relating the surface area  $S_j$  of node  $j$  to the total surface area  $S$  of the tank, thus

$$(UA)_j^{(\text{amb})} = \frac{S_j}{S} (UA)^{(\text{amb})}. \quad (36)$$

## 1.9 PCM modules

Two different geometries for integrated modules consisting of PCM into the storage tank can be treated with the present storage model.

- (i) Cylindrical rods consisting of PCM (see Sec. 1.9.1)
- (ii) Spheres consisting of PCM (see Sec. 1.9.4)

### 1.9.1 Cylindrical Rods

The geometry of one PCM module is depicted in Fig. 7. It is a hollow cylinder with inner radius  $R_i$  and outer radius  $R_o$ , where the inner radius can be set to zero resulting in a filled cylinder of radius  $R_o$ . The number of radial nodes is given by  $n_r$ . Fig. 8 shows the arrangement of PCM modules inside the storage tank. In total there are  $N_{\text{PCM}}$  modules, each having the volume  $V_{\text{PCM}}$  and the surface area  $A_{\text{PCM}}$ . The position of the PCM modules inside the storage tank is given by the node numbers  $t_{\text{PCM}}$  and  $b_{\text{PCM}}$  defining the top and bottom extension of the modules, respectively. Node  $j$  and radial node  $r$  of the PCM

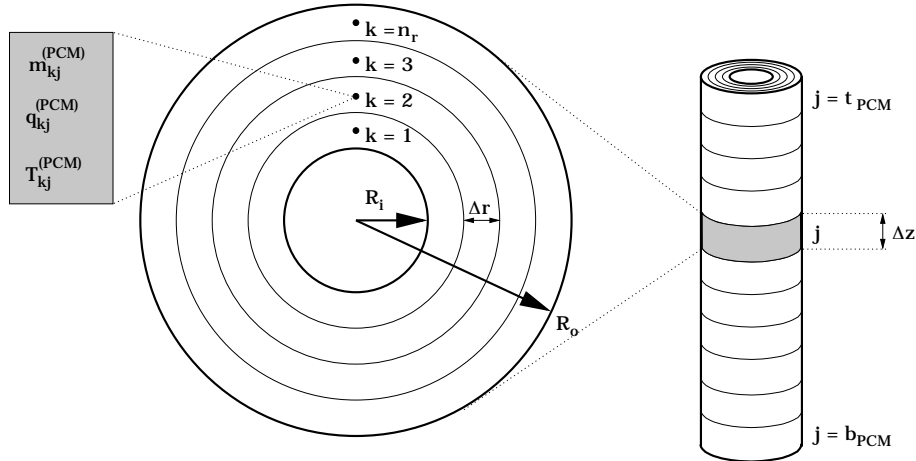


Figure 7: Geometry of one PCM module as hollow cylinders of inner radius  $R_i$  and outer radius  $R_o$ .

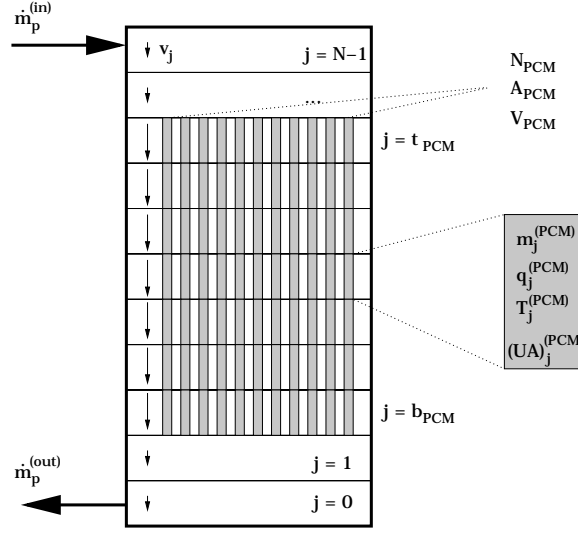


Figure 8: The arrangement of the cylindrical PCM modules inside the storage tank.

module is characterized by its mass,  $m_{kj}^{(\text{PCM})}$ , its specific enthalpy  $q_{kj}^{(\text{PCM})}$ , and  $T_{kj}^{(\text{PCM})}$  its corresponding temperature. The heat transfer rate between the PCM node  $j$  and storage node  $j$  is denoted by  $(UA)_i^{(\text{PCM})}$  for the inner surface and  $(UA)_o^{(\text{PCM})}$  for the outer surface. With these conventions, the energy change of storage node  $j$  due to the PCM modules is given by

$$\dot{Q}_j^{(\text{PCM})} = -N_{\text{PCM}} \left\{ (UA)_i^{(\text{PCM})} [T_j - T_{1j}^{(\text{PCM})}] + (UA)_o^{(\text{PCM})} [T_j - T_{n_r,j}^{(\text{PCM})}] \right\}. \quad (37)$$

In order to obtain the node temperature of the PCM module we have to solve the heat equation for the PCM modules for which we take cylindrical coordinates and assume no dependence on the angular coordinate,

$$\rho \frac{\partial(c_p T)}{\partial t} = \lambda \Delta T. \quad (38)$$

To arrive at the discretized form of the above equation we introduce the mesh points  $(r_k, z_j)$  (compare Fig. 7)

$$r_k = R_i + (k-1)\Delta r \quad (39)$$

$$z_j = j\Delta z \quad (40)$$

which we abbreviate by the index pair  $kj$  in following discussion. If we integrate both sides of (38) over the volume

$$\int_{\Omega} d^3r = \int_k^{k+1} r dr \int_j^{j+1} dz \int_0^{2\pi} d\phi \quad (41)$$

and use the Gauss integral theorem on the left hand side

$$\int_{\Omega} d^3r \vec{\nabla} \cdot \vec{F} = \oint_{\partial\Omega} \vec{F} \cdot d\vec{A} \quad (42)$$

we obtain the energy balance of the PCM module for the element  $kj$  by which the required enthalpies  $q_{kj}^{(\text{PCM})}$  and temperatures  $T_{kj}^{(\text{PCM})}$  are determined

$$\begin{aligned}
m_{kj}^{(\text{PCM})} \frac{dq_{kj}^{(\text{PCM})}}{dt} &= V_{kj} \lambda^{(\text{PCM})} \left[ \frac{T_{kj+1}^{(\text{PCM})} - 2T_{kj}^{(\text{PCM})} + T_{kj-1}^{(\text{PCM})}}{(\Delta z)^2} \right] \\
&+ V_{kj} \lambda^{(\text{PCM})} \left[ \frac{r_{k+1} \left( T_{k+1j}^{(\text{PCM})} - T_{kj}^{(\text{PCM})} \right) - r_k \left( T_{kj}^{(\text{PCM})} - T_{k-1j}^{(\text{PCM})} \right)}{r_{k+\frac{1}{2}} (\Delta r)^2} \right] \\
&- (UA)_i^{(\text{PCM})} \left[ T_{1j}^{(\text{PCM})} - T_j \right] \\
&- (UA)_o^{(\text{PCM})} \left[ T_{n_rj}^{(\text{PCM})} - T_j \right].
\end{aligned} \tag{43}$$

The first two lines describe the heat conduction to neighboring PCM nodes while the third and fourth lines, respectively, take account of the heat transfer to or from the storage fluid at the inner and outer surface of the PCM modules. Concerning the time evolution, the implicit solution scheme is only working if the time step  $\Delta t$  is chosen smaller than the both of the stability criterions

$$\tau_r = \frac{(\Delta r)^2 \rho c_p}{2\lambda^{(\text{PCM})}} \tag{44}$$

$$\tau_z = \frac{(\Delta z)^2 \rho c_p}{2\lambda^{(\text{PCM})}} \tag{45}$$

The crucial point in the Eqs. (37) and (43) above is of course the determination of the overall heat transfer coefficients  $(UA)_i^{(\text{PCM})}$  and  $(UA)_o^{(\text{PCM})}$ . In a first step we can write them as

$$(UA)_i^{(\text{PCM})} = \frac{2\pi R_i H_{\text{PCM}}}{t_{\text{PCM}} - b_{\text{PCM}} + 1} h_j^i \tag{46}$$

$$(UA)_o^{(\text{PCM})} = \frac{2\pi R_o H_{\text{PCM}}}{t_{\text{PCM}} - b_{\text{PCM}} + 1} h_j^o \tag{47}$$

where the first term is the area of the PCM module at node  $j$  at the inner and outer side, respectively. The remaining heat transfer coefficient  $h_j^i$  and  $h_j^o$  will depend on the velocity  $v_j$  of the storage fluid relative to the PCM modules, thus  $h_j = h_j(v_j)$ . The velocity  $v_j$  of the fluid flow in the storage relative to the PCM module is determined by the mass flow rates  $\dot{m}_p^{(\text{in})}$  at all double ports  $p$ , and the mass  $m_j$  of the storage node  $j$ ,

$$v_j = \frac{\Delta x}{m_j} \sum_p d_p \epsilon_{i_p j o_p} \dot{m}_p^{(\text{in})} \tag{48}$$

where the dimensionless number  $d_p$  and  $\epsilon_{i_p j o_p}$ , respectively, determine the direction of flow and decide whether the considered node  $j$  lies between the in- and outlet of port  $p$  (compare Eqs. (15) and (16)). The following two sections will deal with the calculation of the heat transfer coefficients from the inner and outer surfaces of the PCM module.

### 1.9.2 Heat transfer from the inner surface

The heat transfer coefficient  $h_j^i$  at node  $j$  from the inner surface of the PCM module can be obtained from the local Nusselt number  $Nu_j$

$$h_j^i = \frac{\lambda Nu_j}{D_i}, \quad (49)$$

where  $\lambda$  is the thermal conductivity of the storage medium and  $D_i = 2R_i$  is the inner diameter of the PCM module (compare Fig. 7). The Nusselt number can be interpreted as a dimensionless temperature gradient at the surface. For the case of internal flow in a cylindrical pipe, the Reynolds number  $Re$  which is the ratio between inertia and viscous forces, and the Prandtl number  $Pr$ , the ratio between momentum and thermal diffusivities, are given by

$$Re = \frac{\rho v D_i}{\mu} \quad (50)$$

$$Pr = \frac{\nu}{\alpha} = \frac{\mu c_p}{\lambda}. \quad (51)$$

Here,  $\mu$  is the dynamic viscosity and  $v$  is the flow velocity determined by Eq. (48).

Before continue with the analysis of Eq. (49) we demonstrate the order of magnitude of the involved quantities using example set up given in Fig. 9. Here, we have chose a store diameter of  $D_{\text{store}} = 0.50$  [m], and inner and outer PCM module diameters of  $D_i = 1.5$  and  $D_o = 6.0$  [cm], respectively. In the given arrangement, a total of 33 PCM modules has been placed into the tank. Thus, we obtain a filling ratio  $\chi$  defined as the total cross sectional area of the PCM

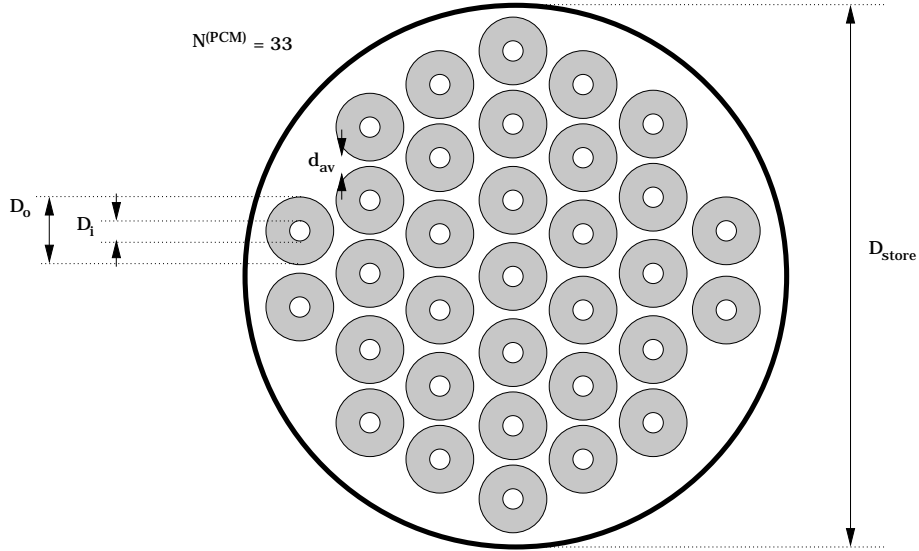


Figure 9: Possible arrangement of the PCM modules inside the storage tank. A total of 33 modules with inner and outer diameters of  $D_i$  and  $D_o$ , respectively, have been placed in the storage tank with diameter  $D_{\text{store}}$ .

modules over the *empty* store cross section of  $\chi = 44$  %. For the storage fluid we take pure water at  $T = 320$  [K], with the thermophysical properties  $\rho = 989$  [kg/m<sup>3</sup>],  $c_p = 4180$  [J/kgK],  $\mu = 577 \times 10^{-6}$  [Ns/m<sup>2</sup>],  $\lambda = 0.64$  [W/mK]. If we assume a mass flow rate of  $\dot{m} = 0.05$  [kg/s] and insert into Eq. (48) we obtain velocity of

$$v = \frac{\dot{m}}{\rho \chi A_{\text{empty-store}}} = \frac{0.05}{989 \times 0.44 \times 0.196} [\text{m/s}] = 0.59 [\text{mm/s}]. \quad (52)$$

Insertion of the above numbers into the expressions for the Reynolds and Prandtl numbers gives,  $Re = 15.2$  and  $Pr = 3.77$ . Thus, the flow conditions are in the laminar regime, and from [1]

$$z_{\text{fd},h} \approx 0.05 D_i Re \quad (53)$$

$$z_{\text{fd},t} \approx 0.05 D_i Re \times Pr \quad (54)$$

the hydrodynamic entry range  $z_{\text{fd},h} = 1.1$  [cm] as well as the thermal entry range  $z_{\text{fd},t} = 4.3$  [cm] can be considered as small compared to the total length of the PCM modules which will be in the order of 1 [m]. Therefore we can safely assume the flow conditions to be fully developed over the whole PCM module hydrodynamically as well as thermally. In this case it can be shown that the Nusselt number  $Nu$  is a constant, independent of  $Re$  and  $Pr$ , as well as of the axial  $z$  location [1], and has the numerical value of

$$Nu = 3.66 \quad (55)$$

Here, we have agreed on isothermal boundary conditions. From Eq. (49) we obtain for the heat transfer coefficient  $k$  using the number in this example  $h_j^i = h^i = 156.2$  [W/m<sup>2</sup>K], and with the inner surface area of  $A_i = D_i \pi L^{\text{PCM}}$ , we finally obtain a value of  $(UA)_i^{(\text{PCM})} = 7.36$  [W/K] per meter PCM module.

### 1.9.3 Heat transfer from the outer surface

In general, the description of the flow conditions and hence the determination of the heat transfer rate  $h^o$  at the outer surface of the PCM module is more complicated than for the inner surface due to the more complex geometry (compare Fig. 9). Nevertheless we make the simple ansatz for the heat transfer rate

$$h^o = \frac{\lambda Nu}{d_{\text{av}}}, \quad (56)$$

in analogy to Eq. (49). Here, we have already omitted the axial dependence of the heat transfer rate since a fully developed hydrodynamical and thermal flow can be expected from what was found from the example in the previous section. In particular the Nusselt number will be a constant and given by Eq. (55). The average distance  $d_{\text{av}}$  between adjacent PCM modules has been defined in the following way

$$d_{\text{av}} = \sqrt{\frac{D_{\text{store}}^2}{N_{\text{PCM}}} - D_o^2}. \quad (57)$$

With the numerical example from the preceeding section, we have  $d_{\text{av}} = 1.1$  [cm], and from (56),  $h^o = 213.4$  [W/m<sup>2</sup>K]. Thus the overall heat transfer rate at the outer surface results in  $(UA)_o^{(\text{PCM})} = 40.2$  [W/K] per meter PCM module.



#### 1.9.4 PCM Spheres

## 2 Description of the program interface

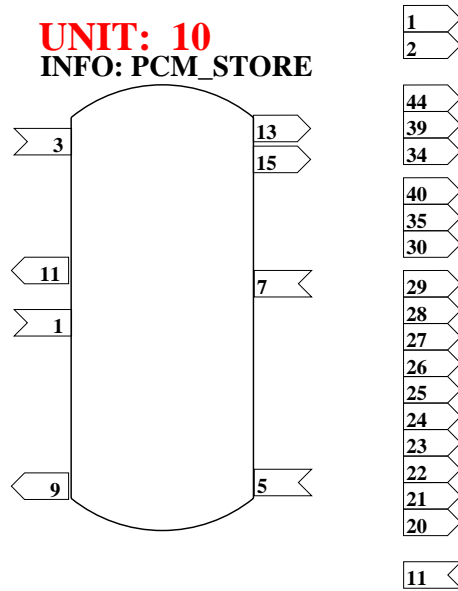


Figure 10: Schematic drawing of the storage model with the most important input and output connections. A full list of all parameters, inputs and outputs is given in Sections 2.1, 2.2 and 2.3.

## 2.1 Parameters

no	Parameters for PCM STORE	Value	Unit
1	volume of storage incl heatexchangers	1	[m <sup>3</sup> ]
2	height of storage	1.5	[m]
3	'kA' ambient losses	10	[W/K]
4	fluid number of storage fluid	0	[-]
5	number n of nodes	10	[]
6	relative position of auxiliary heater (bottom)	0.8	[-]
7	relative position of auxiliary heater (top)	0.9	[-]
8	power of auxiliary heater	5000	[W]
9	start temperature at top of store	20.0	[°C]
10	start temperature at bottom of store	20.0	[°C]
11	number of temp. sensors in tank (max. 10)	10	[-]
12	relative height of first temperature sensor	0.01	[-]
13	relative height of last temperature sensor	0.99	[-]
14	$\lambda_{down-up}$ If 0 : Maximal mixing	0	[W/mK]
15	$\lambda_{conduction}$ If 0 : Calculated from lambda =0.25	2.0	[W/mK]
16	currently not used	0	[-]
17	currently not used	0	[-]
18	currently not used	0	[-]
19	currently not used	0	[-]
20	PORT1 : type : 0 = double port , 1 = int. HX	1	[-]
21	PORT1 : relative height of inlet	0.9	[-]
22	PORT1 : relative height of outlet	0.7	[-]
23	PORT1 : relative height of temperature sensor	0.8	[-]
24	PORT1 : length of int. heat exchanger pipe	4.0	[m]
25	PORT1 : inner diameter of int. heat ex. pipe	10.0	[mm]
26	PORT1 : outer diameter of int. heat ex. pipe	15.0	[mm]
27	PORT1 : thermal conductivity of pipe wall	300	[W/mK]
28	PORT1 : heat transfer coeff., computed if = 0	50.0	[W/Km]
29	PORT1 : currently not used	0	[-]
30	PORT2 : type : 0 = double port , 1 = int. HX	1	[-]
31	PORT2 : relative height of inlet	0.5	[-]
32	PORT2 : relative height of outlet	0.0	[-]
33	PORT2 : relative height of temperature sensor	0.3	[-]
34	PORT2 : length of int. heat exchanger pipe	4.0	[m]
35	PORT2 : inner diameter of int. heat ex. pipe	10.0	[mm]
36	PORT2 : outer diameter of int. heat ex. pipe	15.0	[mm]
37	PORT2 : thermal conductivity of pipe wall	300	[W/mK]
38	PORT2 : heat transfer coeff., computed if = 0	50.0	[W/Km]
39	PORT2 : currently not used	0	[-]

no	Parameters for PCM STORE	Value	Unit
40	PORT3 : type : 0 = double port , 1 = int. HX	1	[-]
41	PORT3 : relative height of inlet	0.0	[-]
42	PORT3 : relative height of outlet	1.0	[-]
43	PORT3 : relative height of temperature sensor	0.5	[-]
44	PORT3 : length of int. heat exchanger pipe	4.0	[m]
45	PORT3 : inner diameter of int. heat ex. pipe	10.0	[mm]
46	PORT3 : outer diameter of int. heat ex. pipe	15.0	[mm]
47	PORT3 : thermal conductivity of pipe wall	300	[W/mK]
48	PORT3 : heat transfer coeff., computed if = 0	50.0	[W/Km]
49	PORT3 : currently not used	0	[-]
50	PORT4 : type : 0 = double port , 1 = int. HX	0	[-]
51	PORT4 : relative height of inlet	0.0	[-]
52	PORT4 : relative height of outlet	0.0	[-]
53	PORT4 : relative height of temperature sensor	0.0	[-]
54	PORT4 : length of int. heat exchanger pipe	4.0	[m]
55	PORT4 : inner diameter of int. heat ex. pipe	10.0	[mm]
56	PORT4 : outer diameter of int. heat ex. pipe	15.0	[mm]
57	PORT4 : thermal conductivity of pipe wall	300	[W/mK]
58	PORT4 : heat transfer coeff., computed if = 0	50.0	[W/Km]
59	PORT4 : currently not used	0	[-]
60	PORT5 : type : 0 = double port , 1 = int. HX	0	[-]
61	PORT5 : relative height of inlet	0.0	[-]
62	PORT5 : relative height of outlet	0.0	[-]
63	PORT5 : relative height of temperature sensor	0.0	[-]
64	PORT5 : length of int. heat exchanger pipe	4.0	[m]
65	PORT5 : inner diameter of int. heat ex. pipe	10.0	[mm]
66	PORT5 : outer diameter of int. heat ex. pipe	15.0	[mm]
67	PORT5 : thermal conductivity of pipe wall	300	[W/mK]
68	PORT5 : heat transfer coeff., computed if = 0	50.0	[W/Km]
69	PORT5 : currently not used	0	[-]
70	Module: geometry: G=0: cylindrical rods, G=1: spheres	0	[-]
71	Module: $N_{PCM}$ number of PCM modules	0	[-]
72	Module: $D_i$ inner diameter of PCM module	1.5	[cm]
73	Module: $D_o$ outer diameter of PCM module	6.0	[cm]
74	Module: $n_r$ number of radial nodes	5	[-]
75	Module: $t_{PCM}$ position in store (top extension)	1.2	[m]
76	Module: $b_{PCM}$ position in store (bottom extension)	0.2	[m]
77	Module: $fl_{PCM}$ fluid number of PCM	0	[-]
78	Module: $\rho_{PCM}$ density of PCM	1000.0	[kg/m <sup>3</sup> ]
79	Module: $\lambda_{PCM}$ thermal conductivity of PCM	1.0	[W/mK]
80	Module: $\lambda_{store}$ thermal conductivity of storage fluid	1.0	[W/mK]
81	Module: $d_c$ Thickness of container material	0.05	[cm]
82	Module: $\lambda_c$ thermal conductivity of container material	0.5	[W/mK]

## 2.2 Inputs

no	Inputs for PCM STORE	Value	Unit
1	PORT1 : PlugInVector	0	[-]
2	PORT1 : currently not used	0	[-]
3	PORT2 : PlugInVector	0	[-]
4	PORT2 : currently not used	0	[-]
5	PORT3 : PlugInVector	0	[-]
6	PORT3 : currently not used	0	[-]
7	PORT4 : PlugInVector	0	[-]
8	PORT4 : currently not used	0	[-]
9	PORT5 : PlugInVector	0	[-]
10	PORT5 : currently not used	0	[-]
11	ambient temperature	20.0	[°C]
12	controller signal for internal auxiliary heater	0	[0..1]

## 2.3 Outputs

no	Outputs for PCM STORE	Value	Unit
1	Total energy of store	.out1	[J]
2	Losses to the ambient	.out2	[J]
3	Energy input by auxiliary heater	.out3	[J]
4	Sum of Energy exchange by PORT1 - PORT5	.out4	[J]
5	currently not used	.out5	[-]
6	' <i>sysgain</i> ' system gains	.out6	[Ws]
7	' <i>sysloss</i> ' system losses	.out7	[Ws]
8	' <i>sysenergy</i> ' internal energy	.out8	[Ws]
9	PORT1 : PlugOutVector	.out9	[-]
10	PORT1 : currently not used	.out10	[-]
11	PORT2 : PlugOutVector	.out11	[-]
12	PORT2 : currently not used	.out12	[-]
13	PORT3 : PlugOutVector	.out13	[-]
14	PORT3 : currently not used	.out14	[-]
15	PORT4 : PlugOutVector	.out15	[-]
16	PORT4 : currently not used	.out16	[-]
17	PORT5 : PlugOutVector	.out17	[-]
18	PORT5 : currently not used	.out18	[-]
19	Mean Temperature of store	.out19	[°C]
20	Temperature at sensor 1	.out20	[°C]
21	Temperature at sensor 2	.out21	[°C]
22	Temperature at sensor 3	.out22	[°C]
23	Temperature at sensor 4	.out23	[°C]
24	Temperature at sensor 5	.out24	[°C]
25	Temperature at sensor 6	.out25	[°C]
26	Temperature at sensor 7	.out26	[°C]
27	Temperature at sensor 8	.out27	[°C]
28	Temperature at sensor 9	.out28	[°C]
29	Temperature at sensor 10	.out29	[°C]



- 3.1 Losses to the ambient
- 3.2 Heating by the built in auxiliary heater
- 3.3 Loading the store by a double port
- 3.4 Test system with three hydraulic connections

## References

- [1] Incropera, F. P., and DeWitt, D. P., *Fundamentals of Heat and Mass Transfer*. John Wiley & Sons, Hoboken, NJ, (2002).
- [2] Petukhov, B. S., in T. F. Irvine and J. P. Hartnett, Eds., *Advances in Heat Transfer*. Vol. 6 Academic Press, New York (1970).
- [3] Gnielinski, V., *Int. Chem. Eng.* **16**, 359 (1976).
- [4] Churchill, S. W., and H. H. S. Chu, *Int. J. Heat and Mass Transfer*. **18**, 1049 (1975).